VOLUME 1, 2018
DOI: 10.31058/j.ac.2018.11003

Effect of Process Conditions on the Catalytic Activity, Structure and Reaction Rate of Impregnated Co-Ni/Al_2O_3 Catalyst for CO Hydrogenation

M. Arsalanfar[1*], M. Fatemi[2], N. Mirzaei[3], M. Abdouss[1], Y. Zamani[4], A. Nouri[5]

[1] Department of Chemistry, Amirkabir University of Technology, Hafez Ave, Tehran, Iran
[2] Department of Chemistry, Faculty of sciences, University of Sistan and Baluchestan, Zahedan, Iran
[3] Department of Chemical and Petroleum Engineering, Sharif University of Technology, Azadi Avenue, Tehran, Iran
[4] Research Institute of Petroleum Industry of the National Iranian Oil Company, Gas Research Division, Tehran, Iran
[5] Department of Chemistry, Islamic Azad University, Shahr-e-Qods Branch, Tehran, Iran

Email Address

maryam_galavy@yahoo.com (M. Arsalanfar)
*Correspondence: maryam_galavy@yahoo.com

Received: 31 May 2018**; Accepted:** 24 June 2018**; Published:** 28 August 2018

Abstract:

The Co-Ni/Al_2O_3 catalyst was prepared using incipient wetness impregnation procedure. The effect of different process conditions including reaction temperature, pressure, H_2/CO feed ratios and Gas Hourly Space Velocity (GHSV) on the catalytic performance of this impregnated catalyst for CO hydrogenation reaction was investigated in a fixed bed micro reactor. For this purpose reaction conditions were changed as follow: H_2/CO ratio from1 to 4, GHSV from 3600 to 6300 and pressure from 1 to 11bar at different temperature from 230 to 260 ℃. Furthermore the rate of CO hydrogenation over the Co-Ni/ Al_2O_3 catalyst was investigated. Characterization of the catalysts was performed using various techniques including XRD, BET, SEM and EDS.

Keywords:

Process Conditions, Co-Ni Catalyst, CO Hydrogenation, Characterization, Reaction Rate

1. Introduction

Fischer-Tropsch Synthesis (FTS) is a well-known process for producing high quality fuels and petrochemicals from synthesis gas (H_2 + CO) which can be easily obtained from other organic resources such as coal, biomass and natural gas [1]. Although several metals are active for FTS, only iron and cobalt catalysts appear to be economically viable on an industrial scale. The higher water-gas shift activity of iron makes it a good candidate for converting hydrogen lean syn gas derived from coal. Controlling selectivity is an important aspect of FTS catalyst development. Typical

cobalt catalysts have a high activity for CO hydrogenation and tend to produce linear alkanes [2]. Cobalt-based FTS catalyst are preferred over Fe-based systems for producing synthetic diesel fuels, since they favor the formation of long-chain *n*-paraffins, are more stable against deactivation by water (a by-product of the FTS reaction), are less active for the competitive water gas-shift (WGS) reaction, and produce less oxygenates [3–5]. Typically, the preparation of Co-based FTS catalysts involves the impregnation of a cobalt precursor salt over a porous inorganic solid, followed by calcination and reduction. Typical supports used for dispersing cobalt in FTS catalysts are amorphous SiO_2, Al_2O_3, and to a lesser extent TiO_2 [6]. It has been reported the selectivity to low molecular hydrocarbons is basically increased with the increase of reaction temperature and inlet H_2/CO ratio, while the selectivity to high molecular hydrocarbons is basically increased with the decrease of total pressure [7]. Some investigators have reported the effect of operation parameters on the product distribution from cobalt-based catalysts [8–18] and showed that the olefin contents of the product spectrum decreased with increasing pressure, which was consistent with previous investigations [19–21].

The aim of the present work is to investigate the effect of process conditions including the inlet H_2/CO feed ratio, GHSV and reaction pressure at various reaction temperatures on the catalytic activity of impregnated Co-Ni/Al_2O_3 catalyst. On the other hand we also attempt to investigate the effect of these process conditions on the CO consumption rate. Catalyst characterization was performed using XRD, BET, SEM and EDS.

2. Experimental Section

2.1. Catalyst Preparation

The used catalysts were prepared by incipient wetness impregnation of Al2O3 with aqueous cobalt nitrate Co (NO3)2.6H2O (0.5M) (99% Merck) and nickel nitrate Ni (NO3)2.6H2O (0.5M) (99% Merck) solutions. The Al2O3 support was first calcined at 600 ℃ in flowing air for 6h before impregnation. For 80%Co-20%Ni/90wt%Al2O3 catalyst, calculated amounts of cobalt nitrate and nickel nitrate were dissolved in distillate water and directly impregnated into the alumina support using incipient wetness. The obtained suspension was then rotated and aged for 4h in a rota-evaporator at 60 ℃. The aged suspension was then filtered, followed by drying at 120 ℃ for 16h to give a material, and hereafter referred to as the catalyst precursor. In order to obtain the final calcined catalyst, the precursor was then calcined in a furnace at 550 ℃ for 6h under the static air.

2.2. Catalysts Characterization

2.2.1. X-Ray Diffraction (XRD)

XRD analysis technique was used to determine the crystalline phases present in the precursor and calcined supported Fe-Co-Mn catalysts (before and after the test). The catalyst specimen was loaded on a sample holder; all samples analyzed on a Bruker AXS D8 Advance diffractometer using monochromatized CuKα radiation at 40 kV, 30 mA, selecting a scan range of $4^\circ < 2\theta < 70^\circ$. Different present phases were identified by matching experimental patterns to entries in Diffract plus version 6.0 indexing software.

2.2.2. BET Measurements

BET surface areas, pore volumes and average pore sizes of the precursor and fresh calcined samples were measured by N2 physisorption using a Quantachrome Nova 2000 automated system (USA). Each catalyst sample was degassed under nitrogen atmosphere at 300 ℃ for 3h. In order to obtain the BET surface areas, pore volumes and average pore sizes, different samples were evacuated at -196 ℃ for 66 minutes.

2.2.3. Scanning Electron Microscopy (SEM) and Energy Dispersive X-Ray Spectrometer (EDS)

The morphology of the catalysts and their precursors was observed by means of a Cambridge S-360 scanning electron microscope instrument (made in England) operating at 20 KV coupled to an energy dispersive x-ray spectrometer (EDS). The samples were coated with gold/palladium for 80s in 20s intervals before the measurements to avoid charging problems.

2.3. Catalyst Testing

Figure1 shows the schematic lay out of experimental setup. The dichotomous stainless steel single tubular vertical fixed bed micro reactor was used; the length of the tube was 360 mm with inner diameter of 20 mm. the reactor is mounted inside a tubular furnace (Atbin, Model ATU 150-15) capable of producing temperature up to 1500 ℃ and controlled by a digital programmable controller (DPC). The alumina jacket is surrounded the tubular micro reactor in order to provide a uniform wall temperature along the length of the reactor. Preheating zone ahead of the catalyst packing and also the beneath zone of the catalyst bed were filled with inert quartz glass beads. The required amount of the meshed catalyst (1.0 g) was held in the middle of the reactor using quartz wool. An electronic back pressure regulator was used, which can control the total pressure of the desired process using a remote control via integration with the TESCOM software package, which can improve or modify its efficiency; it is capable of working on pressures ranging from atmospheric pressure to 100 bar. The temperature of all of different different zones include: preheating zone, catalyst bed and underneath zone of the reactor is checked by three separate thermocouples placed in different parts of the reactor. The thermocouple which controls bed temperature is placed exactly below the catalyst bed. The inlet feed gas is arrived from top of the reactor and the outlet products are avoided from underside of the reactor. Three mass flow controllers (Brooks, Model 5850E) equipped with a four-channel read out and control equipment (Brooks 0154) were used to adjust automatically the flow rate of the inlet gases (CO, H2, and N2 with purity of 99.999%). The catalytic reactor bed was purged by nitrogen gas and then the reduction process was carried out at atmospheric pressure under a flowing H2-N2 stream (H2/N2=1, flow of each gas =30ml/min) at 400 ℃ for 12h before synthesis gas exposure. The CO hydrogenation was carried out under different reaction conditions of T= 230 to 260 ℃, P= 1 to 11 bar, H2/CO= 1/1 to 4/1 and GHSV= 3600–6300 h-1. In each test, 1.0 g catalyst was loaded and the reactor operated about 12 h to ensure steady state operations were attained. Reactant and product streams were analyzed on-line using a gas chromatograph (Thermo ONIX UNICAM PROGC+) equipped with sample loop, two Thermal Conductivity Detectors (TCD) and one Flame Ionization Detector (FID) able to perform the analysis of a wide variety of gaseous hydrocarbon mixtures, one TCD used for the analysis of hydrogen and the other one used for all the permanent gases such as N2, O2 and CO. The FID is

used for the analysis of hydrocarbons. The system is applicable to the analysis of non-condensable gases, methane through C8 hydrocarbons. The contents of the sample loop were injected automatically into an alumina capillary column (30m×0.550mm). Helium was employed as a carrier gas for optimum sensitivity (flow rate=30ml/min). The GC calibration was carried out using various calibration mixtures and pure compounds obtained from American Matheson Gas Company (USA).

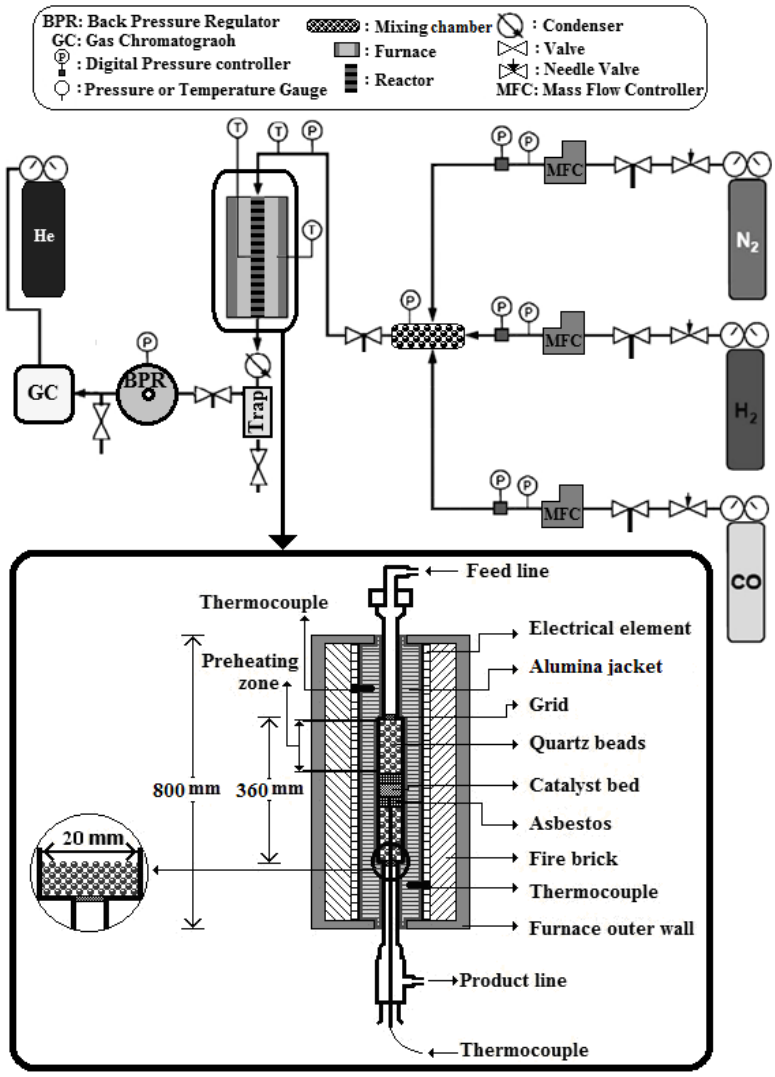

Figure 1. *Schematic representation of the reactor in a flow diagram used.*

3. Catalyst Screening Results

Characterization of the precursor and calcined catalysts was carried out using different techniques. Characterization of the catalyst precursor and calcined sample before the test was carried out using XRD and the obtained patterns are displayed in Figure 2. In the case of precursor, a high background in the low angle region revealed the presence of an amorphous in the diffraction pattern due to indiscriminate scattering of X-rays. Consequently, other phases that may be poorly crystalline or have small crystallite size, and hence broader peaks, are more difficult to detect. The actual identified phases in the calcined catalyst before the CO hydrogenation test, were found to be Co_3O_4 (cubic), NiO (cubic) and $NiCo_2O_4$ (cubic). The XRD results showed that calcination process leads to phase changes of the catalyst precursor into

more thermodynamically stable oxidic phases in the calcined sample. The schematic lay out of this phase changes process is illustrated in Figure 3.

The BET measurements were used in order to measure the specific surface area, pore volume and average pore size of the catalyst. The BET results of the catalyst precursor

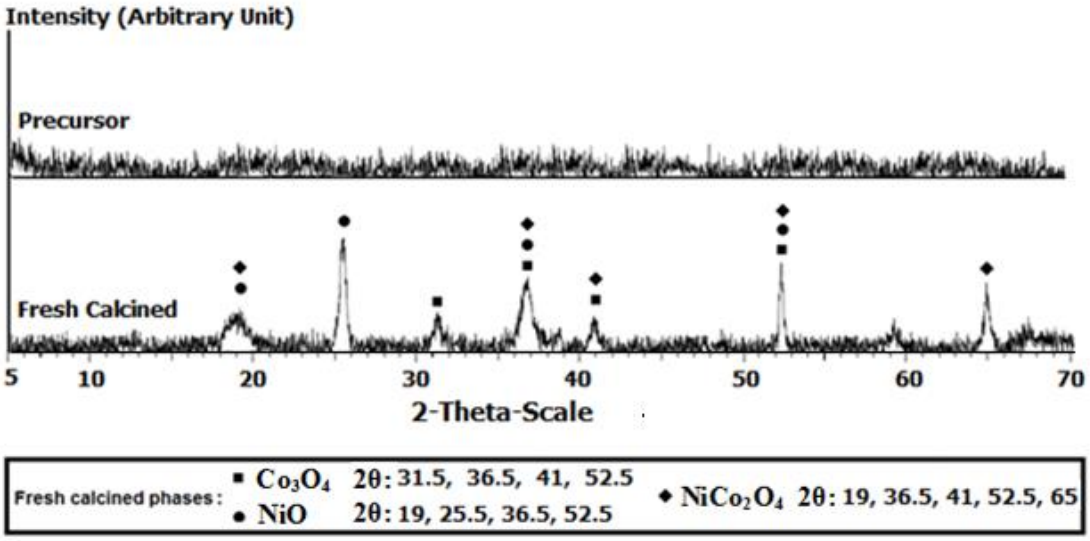

Figure 2. *XRD patterns of the catalyst precursor and calcined sample.*

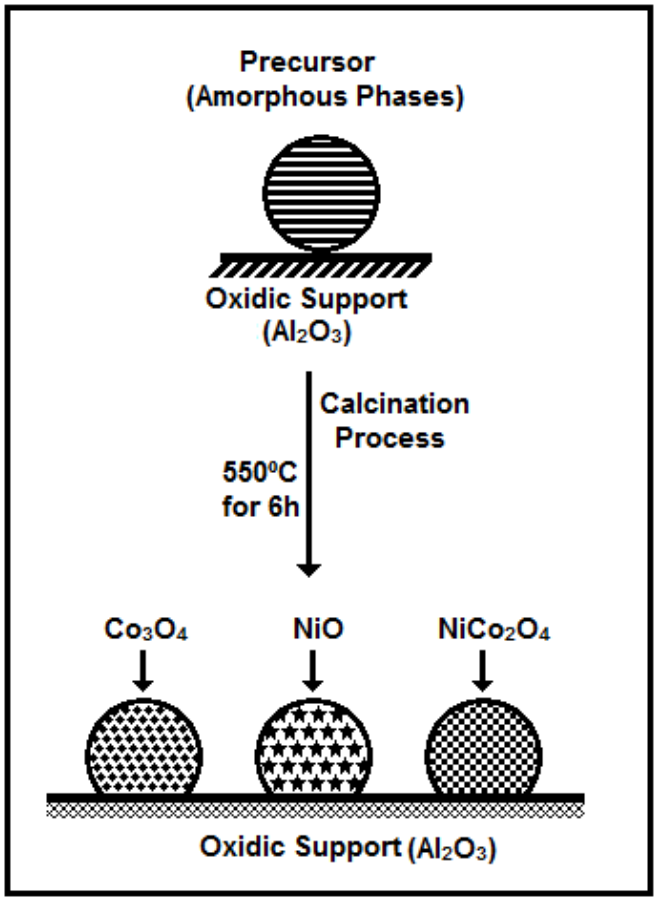

Figure 3. *Schematic representation of phase changes during calcination process.*

and fresh calcined catalyst are presented in Table 1.

Table 1. *BET results of Co-Ni/Al2O3 catalyst in states of precursor and calcined.*

Sample	SSA (m^2/g)	PV (cm^3/g)	PS (A °)
Precursor	104.00	0.05	23.13
Fresh calcined	90.59	0.04	24.20

SSA: Specific Surface area
PV: Pore volume
PS: Pore Size

As it observed, the catalyst precursor has a higher specific surface area (104.00m^2/g) than the calcined catalyst before the test (90.59m^2/g). The BET results also showed that the porosity (pore size and pore volume) of the catalyst precursor and calcined samples was changed and the catalyst precursor has higher pore volume and lower pore size in comparison with the calcined sample.

The SEM method was used in order to investigate the morphological properties and structural changes in different states of precursor and calcined samples. The obtained electron micrographs presented in Figure 4 showed that the catalyst precursor and calcined samples have different morphological features. These images showed that the catalyst precursor is comprised of irregularly shaped grains with different sizes and low dense agglomeration; this sample has disproportionate morphology (Figure 4a). The calcination process at 550 ℃ for 6h leads to changes in morphological features of calcined sample. The fresh calcined sample is comprised of the particles with different sizes and large grains are embedded in mixture of small grains. The SEM images of the calcined samples showed that the size of particles is reduced in comparison with the precursor and agglomeration of the particles is increased in the calcined sample (Figure 4b).

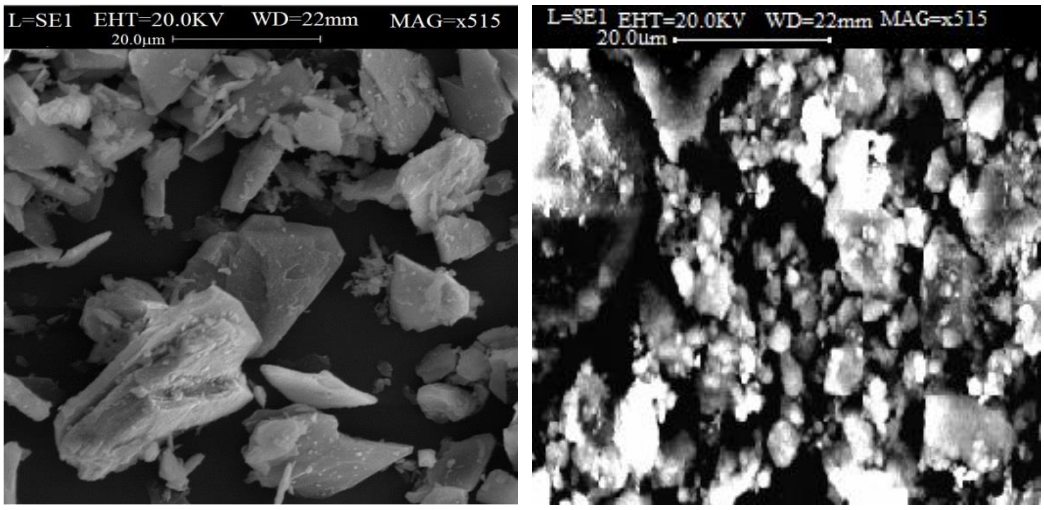

Figure 4. *SEM images of Co-Ni/Al2O3 catalyst in (a) precursor and (b) calcined catalyst.*

The EDS characterization was also carried out at different cases of catalysts (precursor and fresh calcined) in order to determine the mean element proportions of the samples. The elemental compositions of the precursor and fresh calcined catalysts obtained from the EDS data are given in Table 2. The EDS spectra of the precursor and calcined samples are also illustrated in Figure 5. The EDS spectrum of the precursor showed the presence of N, O, Al, Ni and Co (Table 2 and Figure 5a) according to the X-ray diffraction data, the XRD pattern of the precursor showed the amorphous phase which makes undetectable these phases. The EDS spectrum of fresh calcined catalyst refers to the presence of O, Al, Ni and Co (Table 2 and Figure 5b), which confirms that this material is comprised of oxidic phases of cobalt and nickel.

This result is supported by the X-ray diffraction data, which showed the existence of Co3O4 (cubic), NiO (cubic) and NiCo2O4 (cubic) phases.

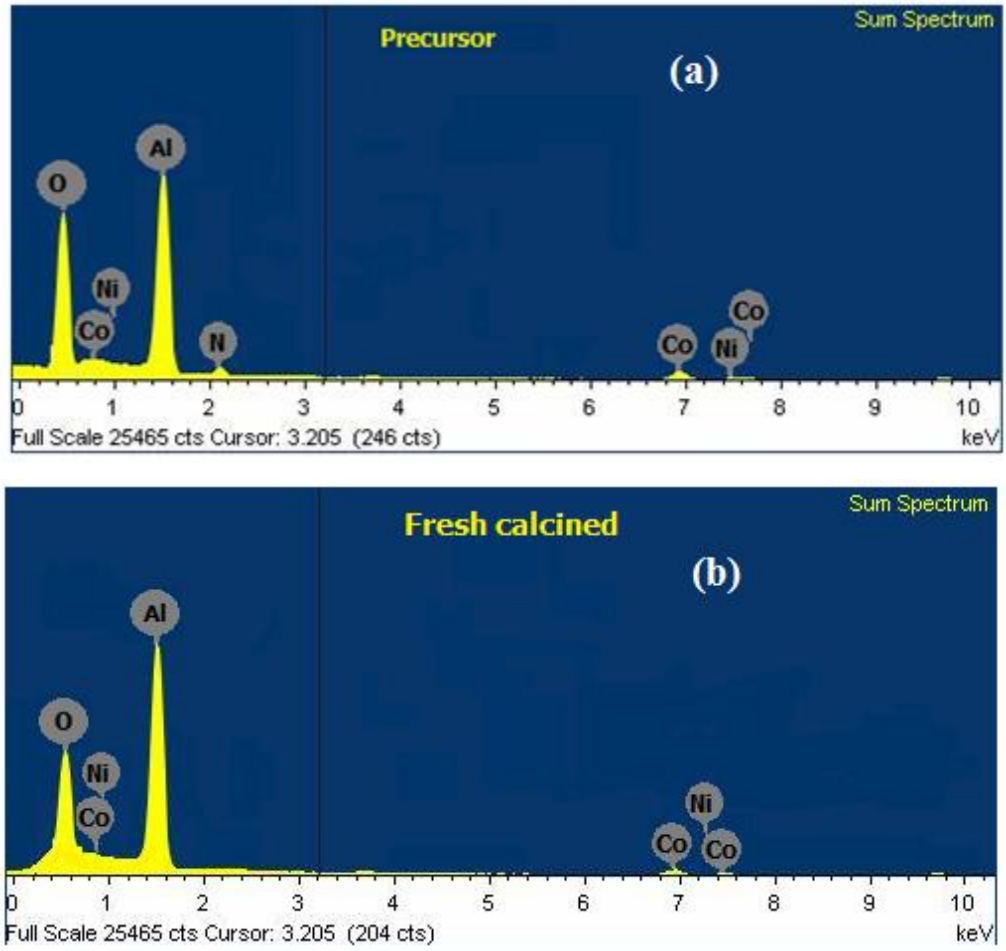

Figure 5. *EDS spectrums of Co-Ni/Al2O3 catalyst in (a) precursor and (b) calcined catalyst.*

Table 2. *EDS data of Co-Ni/Al2O3 catalyst in precursor and calcined states.*

Catalyst	Elements	Weight%	Atomic%
Precursor	N	0.85	0.57
	O	40.07	55.59
	Al	48.45	39.85
	Co	8.42	3.35
	Ni	2.21	0.64
Calcined catalyst	O	42.53	65.62
	Al	51.32	32.25
	Co	4.75	1.65
	Ni	1.41	0.49

4. Effect of Process Conditions on the CO Consumption Rate and CO Conversion

Operational conditions have a great effect on the CO conversion and CO consumption rate. So that, after determining the optimum kinetic rate equation and FTS mechanism on the Al_2O_3 supported Co-Ni catalyst in our previous work [22], we attempt to investigate and vindicate some operational conditions effects on the CO conversion and consumption rate. In order to investigate the effect of operational conditions on the catalyst activity and CO consumption rate the H_2/CO feed ratio,

GHSV and reaction pressure were changed at different reaction temperature of 230-260 ℃.

Feed ratio effect: It was found that the H_2/CO feed ratio has significant effects on the CO hydrogenation reaction. The influence of the reaction H_2/CO feed molar ratio on the CO conversion was investigated in the reaction conditions of GHSV=4500h^{-1}, p=1atm at T=230-260 ℃. The reduced catalyst was tested at each feed ratio for 12h and the obtained results are displayed in Figure 6.

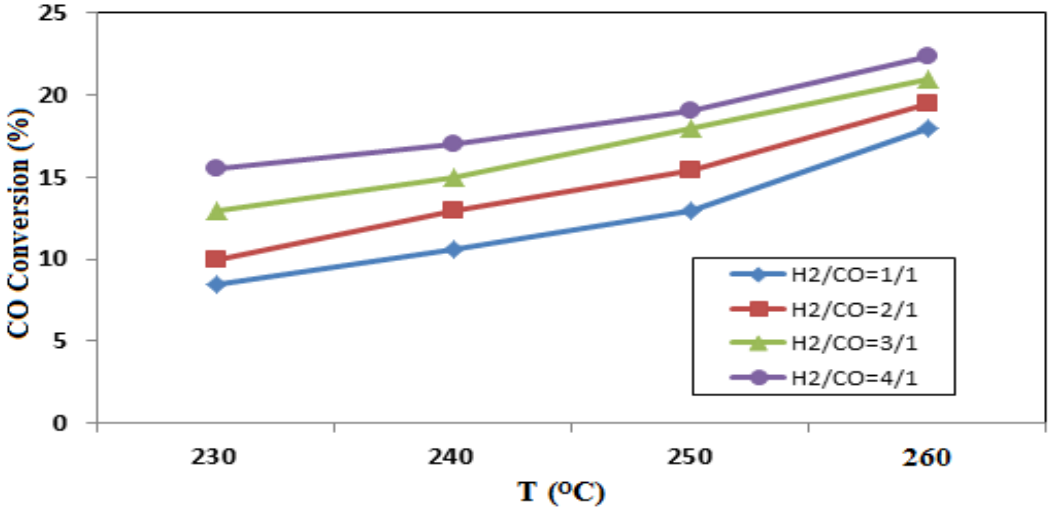

Figure 6. *Effect of H2/CO feed ratio on the CO conversion at different temperatures (230-260 ℃).*

As it can be seen in this Figure, at all temperatures the same trend for CO conversion was observed with increasing the H_2/CO ratio; in the certain temperature along with increasing the H_2/CO ratios from 1/1 to 4/1 the CO conversion is increased. This Figure also shows that in the certain ratio of H_2/CO along with increasing the reaction temperature from 230 to 260 ℃ the CO conversion is increased. The effect of the H_2/CO feed ration was also investigated on the CO consumption rate at different temperatures (230-260 ℃), and the obtained results are plotted in Figure 7.

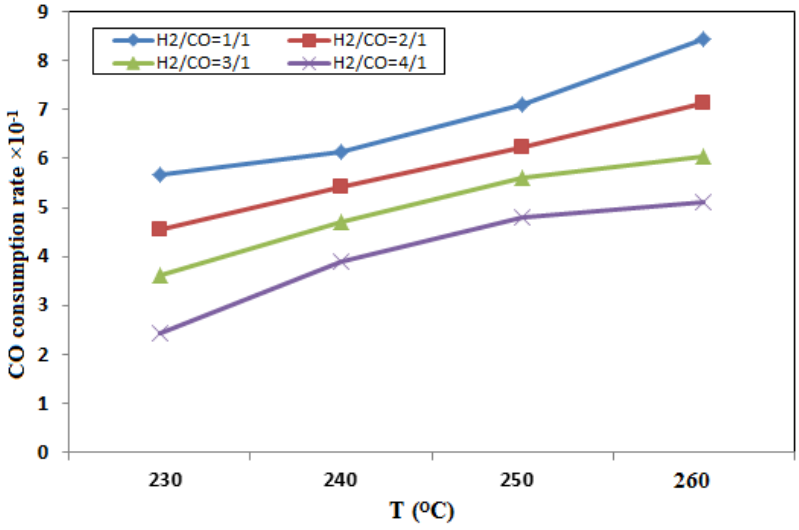

Figure 7. *Effect of H_2/CO feed ratio on the CO consumption rate at different temperatures (230-260 ℃).*

According to these results with increasing the H_2/CO feed ratio the CO consumption rate was decreased at each temperature. This figure also shows that in the certain feed ratio along with increasing the reaction temperature CO consumption rate is increased. In the previous work [22] the CO hydrogenation mechanism and rate equation over the Co-Ni catalyst were obtained; according to the best fitted model the rate equation was obtained as follow:

$$-r_{CO} = \frac{k_p \cdot b_{CO} \cdot P_{CO} \cdot b_{H_2} \cdot P_{H_2}}{\left(1 + b_{CO} \cdot P_{CO} + b_{H_2} \cdot P_{H_2}\right)^2} \quad (1)$$

This rate equation shows that CO hydrogenation over this catalyst is performed according to the Langmuir-Hinshelwood-Hougen-Watson (LHHW) type rate equation, and in the best fitted model, both H_2 and CO were adsorbed and activated on the catalyst surface. Along with increasing the H_2/CO ratio the concentration of H_2 is increased over the catalyst surface and hence over the active sites. Therefore, the number of adsorbed CO molecules on the active sites of the catalyst surface is decreased and so the CO consumption rate is decreased.

GHSV effect: In order to investigate the effect of space velocity on the CO conversion and consumption rate, a series of experiments were carried out at different GHSV from 3600 to 6300h^{-1} under the atmospheric pressure, H_2/CO=2/1 and different temperature of 230-260 ℃. The effects of GHSV on the CO conversion at different temperatures are plotted in Figure 8.

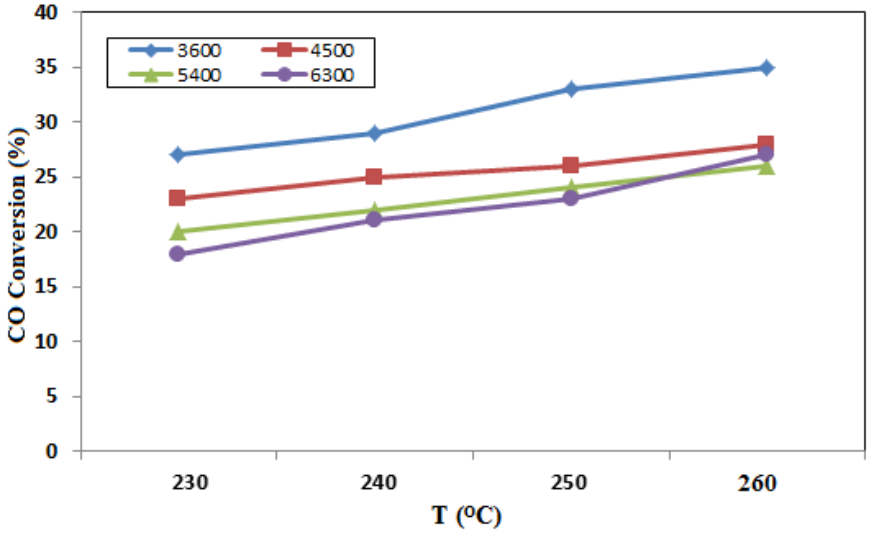

Figure 8. *Effect of GHSV on the CO conversion at different temperatures (230-260 ℃).*

This Figure shows that with increasing the GHSV from 3600 to 6300h-1, in each temperature the CO conversion is decreased. Along with increasing the space velocity the residence time of reactants and products in the reactor is decreased and so the CO conversion is decreased. Figure 8 also shows that with increasing the reaction temperature, in each space velocity, the CO conversion is enhanced.

The effect of GHSV was also investigated on the CO consumption rate and the obtained results are displayed in Figure 9.

DOI: 10.31058/j.ac.2018.11003

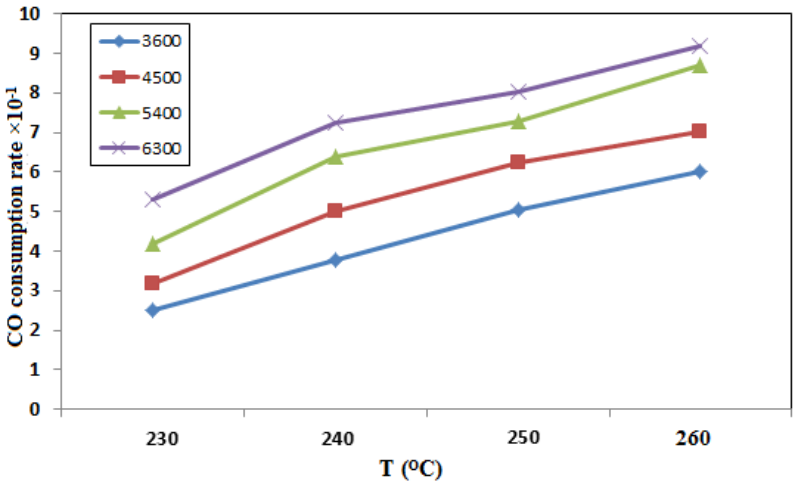

Figure 9. *Effect of GHSV on the CO consumption rate at different temperatures (230-260 ℃).*

As it shown, with increasing the GHSV from 3600 to 6300h^{-1} the CO consumption rate is increased. On the other hand, along with increasing the reaction temperature, at each GHSV, the consumption rate of CO is enhanced.

Pressure effect: The reaction pressure is an important parameter for CO hydrogenation and variation of pressure leads to different products. The catalytic behavior for CO hydrogenation at atmospheric pressure is different with high pressure. Higher pressures and higher carbon monoxide conversions would probably lead to saturation of catalyst pores by liquid reaction products [23]. The effect of total reaction pressure on the CO conversion over the Co-Ni/Al_2O_3 catalyst under the H_2/CO=2/1, GHSV=4500h^{-1} at different temperatures of 230-260 ℃ was investigated and the obtained results are presented in Figure 10.

As can be observed, along with increasing the total reaction pressure, at each temperature, the CO conversion is increased. Malek Abbaslou et al [24] reported that along with increasing the pressure, the supercritical media exposes a liquid-like density, which can raise elicitation from the catalyst pores. This phenomenon increases the adsorption of CO and H2 molecules on the catalyst active sites and hence increases the CO conversion. The Figure 10 also shows that along with increasing the reaction temperature, under each reaction pressure, the CO conversion is increased.

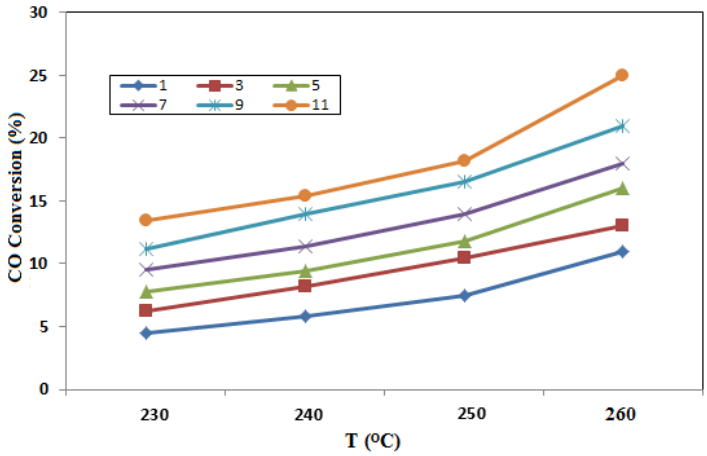

Figure 10. *Effect of reaction pressure on the CO conversion at different temperatures (230-260 ℃).*

The effect of the reaction pressure on the CO consumption rates was also investigated and the obtained results are presented in Figure 11.

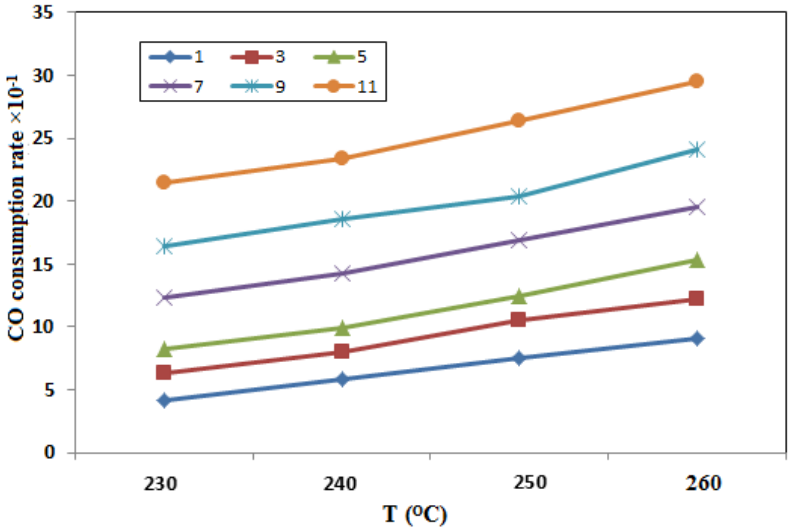

Figure 11. *Effect of reaction pressure on the CO consumption rate at different temperatures (230-260 ℃).*

These results show that with increasing the total reaction pressure the CO consumption rate is increased, but this increasing trend after the reaction pressure of 5bar is rigorous. It has been reported that with increasing the pressure, the increasing of CO conversion leads to elevate the active surface carbon species, and ameliorate encounter eventuality of the catalysts and reactants; so that the reaction rate is increased [25]. Figure 11 also shows that with increasing the reaction temperature the CO consumption rate is enhanced, in each reaction pressure.

5. Conclusions

The Co-Ni/Al_2O_3 catalyst was prepared using incipient wetness impregnation procedure. The effect of operational conditions including H_2/CO feed ratio, Gas Hourly Space Velocity (GHSV) and reaction pressure at different reaction temperatures of 230-260 ℃ on the CO conversion and CO consumption rate were investigated. The obtained results show that all investigated operational parameters have influenced the CO conversion and hence have influenced the CO consumption rate. The obtained results are in good agreement with the obtained results in our previous work [22] and the reported results in the literatures [23-25]. Characterization results obtained from various techniques show that the catalyst structure, porosity, phases and morphology are completely different in the cases of precursor and calcined catalyst, and strongly affected by calcination process.

Conflicts of Interest

The authors declare that there is no conflict of interest regarding the publication of this article.

References

[1] Cho K. M.; Park S.; Seo J. G.; Youn M. H.; Nam I.; Baeck S-H.; Chung J. S.; Jun K-W.; Song I. K. Effect of calcination temperature of alumina supports on the wax

hydrocracking performance of Pd-loaded mesoporous alumina xerogel catalysts for the production of middle distillate. *Chem. Eng. J.* 2009, 146, 307-314.

[2] Pendyala V. R. R.; Jacobs G.; Mohandas J. C.; Luo M.; Hamdeh H. H.; Ji Y.; Ribeiro M. C.; Davis B. H.; Fischer–Tropsch Synthesis: Effect of Water Over Iron-Based Catalysts. *Catal. Lett*, 2010, 140, 98-105.

[3] Concepción P.; López C.; Martínez A.; Puntes V. F.; Characterization and catalytic properties of cobalt supported on delaminated ITQ-6 and ITQ-2 zeolites for the Fischer–Tropsch synthesis reaction. *J. Catal, 2004*, 228, 321-332.

[4] Fleisch T. H.; Sills R. A.; Briscoe M. D.; Emergence of the Gas-to-Liquids Industry: a Review of Global GTL Developments. *J. Nat. Gas. Chem*, 2002, 11, 1-14.

[5] Van Berge P. J.; Barradas S.; Van De Loodsrecht J.; Visagie J. L. Advances in the cobalt catalyzed Fischer-Tropsch synthesis. *Erdoel, Erdgas, Kohle,* 2001, 117, 138-142.

[6] Oukaci R.; Singleton A. H.; Goodwin Jr J. G. Comparison of patented Co F–T catalysts using fixed-bed and slurry bubble column reactors. *Appl. Catal. A: Gen.* 1999, 186, 129-144.

[7] Liu Y.; Teng B.; Guo X.; Li Y.; Chang J.; Tian L.; Hao X.; Wang Y.; Xiang H.-W.; Xu Y.-Y.; Li Y.-W. Effect of reaction conditions on the catalytic performance of Fe-Mn catalyst for Fischer-Tropsch synthesis. *J. Mol. Catal. A: Chem*, 2007, 272, 182-190.

[8] Keyser M. J.; Eversion R. C.; Espirnoza R. L. Fischer-Tropsch Kinetic Studies with Cobalt. Manganese oxide Catalyst. *Ind. Eng. Chem. Res,* 2000, 39, 48-54.

[9] Tao Z.; Yang Y.; Zhang C.; Li T.; Wang J.; Wan H.; Xiang H.; Li Y. Effect of calcium promoter on a precipitated iron–manganese catalyst for Fischer–Tropsch synthesis. *Catal. Com*, 2006, 7, 1061-1066.

[10] Zhang C. H., Yang Y., Teng B.-T., Li T.-Z., Zheng H.-Y., Xiang H.-W., Li Y.-W., Study of an iron-manganese Fischer–Tropsch synthesis catalyst promoted with copper. *J. Catal*, 2006, 237, 405-415.

[11] Das D.; Ravichandran G.; Chakrabarty D. K. Synthesis of light alkenes from syngas on silicalite-1 supported cobalt and cobalt-manganese catalysts. *Appl. Catal. A: Gen.* 1995, 131, 335-345.

[12] Ajamein H.; Sarkari M.; Fazlollahi F.; Atashi H. Effects of Reaction Conditions on Cobalt-Catalyzed Fischer-Tropsch Synthesis: Interactions between Operating Factors. *J. Korean. Chem. Soc*, 2011, 55, 824-829.

[13] Jiang M.; Koizumi N.; Ozaki T.; Yamada M. Adsorption properties of cobalt and cobalt-manganese catalysts studied by in situ diffuse reflectance FTIR using CO and CO+H_2 as probes. *Appl. Catal. A:Gen,* 2001, 209, 59-70.

[14] Malessa R.; Baerns M. Iron/manganese oxide catalysts for Fischer-Tropsch synthesis. 4. Activity and selectivity. *Ind. Eng. Chem. Res*, 1988, 27, 279-283.

[15] Bian G.; Oonuki A.; Koizumi N.; Nomoto H.; Yamada M. Studies with a precipitated iron Fischer-Tropsch catalyst reduced by H_2 or CO. *J. Mol. Catal. A: Chem*, 2002, 186, 203-213.

[16] Morales F.; de Smit E.; de Groot F. M. F.; Visser T. Weckhuysen B. M., Effects of manganese oxide promoter on the CO and H_2 adsorption properties of titania-supported cobalt Fischer–Tropsch catalysts. *J. Catal*, 2007, 246, 91-99.

[17] Li H.; Wang S.; Ling F.; Li J. Studies on MCM-48 supported cobalt catalyst for Fischer–Tropsch synthesis. *J. Mol. Catal. A: Chem*, 2006, 244, 33-40.

[18] Sun S.; Tsubaki N.; Fujimoto K. The reaction performances and characterization of Fischer–Tropsch synthesis Co/SiO_2 catalysts prepared from mixed cobalt salts. *Appl. Catal. A: Gen*. 2000, 202, 121-131.

[19] Park C.; Baker R. T. K.; Carbon Deposition on Iron–Nickel During Interaction with Ethylene–Carbon Monoxide–Hydrogen Mixtures. *J. Catal*, 2000, 190, 104-117.

[20] Kim S.-M., Bae J. W., Lee Y-J., Jun K-W., Effect of CO_2 in the feed stream on the deactivation of $Co/\gamma\text{-}Al_2O_3$ Fischer–Tropsch catalyst. *Catal. Com*, 2008, 9, 2269-2273.

[21] Arsalanfar M.; Mirzaei A. A.; Bozorgzadeh H. R.; Atashi H. Effect of process conditions on the surface reaction rates and catalytic performance of MgO supported Fe–Co–Mn catalyst for CO hydrogenation. *J. Ind. Eng. Chem*, 2012, 18, 2092-2102.

[22] M. Arsalanfar; M. Fatemi; N. Mirzaei; M. Abdouss; E. Rezazadeh; Y. Zamani, accepted for publication in the Journal of Progress in Reaction Kinetics and Mechanism *[manuscript ID: PRK1700633]*

[23] Li T.; Yang Y.; Tao Z.; Zhang C.; Xiang H.; Li Y. Study on an iron manganese Fischer–Tropsch synthesis catalyst prepared from ferrous sulfate. *Fuel. Process. Technol.* 2009, 90, 1247-1251.

[24] Malek Abbaslou R. M.; Slotan Mohammadzadeh J. S.; Dalai A. K. Review on Fischer–Tropsch synthesis in supercritical media. *Fuel. Process. Technol*, 2009, 90, 849-856.

[25] Liu Y.; Teng B.; Guo X.; Li Y.; Chang J.; Tian L.; Hao X.; Wang Y.; Xiang H-W.; Xu Y-Y.; Li Y-W. Effect of reaction conditions on the catalytic performance of Fe-Mn catalyst for Fischer-Tropsch synthesis. *J. Mol. Catal. A: Chem*, 2007, 272, 182-190.